Model family of high-temperature superconductors: $Tl_mCa_{n-1}Ba_2Cu_nO_{2(n+1)+m}$ ($m=1,2$; $n=1,2,3$)

S. S. P. Parkin, V. Y. Lee, A. I. Nazzal, R. Savoy, T. C. Huang, G. Gorman, and R. Beyers
IBM Research Division, Almaden Research Center, 650 Harry Road, San Jose, California 95120-6099
(Received 31 May 1988)

We describe the structures and superconducting properties of six compounds in the Tl-Ca-Ba-Cu-O system of the general form, $Tl_mCa_{n-1}Ba_2Cu_nO_{2(n+1)+m}$, where $m=1$ or 2 and $n=1$, 2, or 3. One of the compounds displays the highest known superconducting transition temperature, $T_c \simeq 125$ K. The structures of these compounds consist of copper perovskitelike blocks containing 1, 2, or 3 CuO_2 planes separated by one or two Tl-O layers and thus form a model family of structures in which both the size and separation of the copper oxide blocks can be independently varied. The superconducting transition temperature increases with the number of CuO_2 planes in the perovskitelike block for both the Tl-O monolayer and bilayer compounds. For each pair of compounds ($m=1,2$) with the same number of CuO_2 planes (same n), the transition temperatures are similar but are consistently 15–20 K lower in the materials with single Tl-O layers. Variations in the transition temperatures in the double and triple CuO_2-layer compounds are observed to correlate with increased densities of intergrowths of related structures.

Recently[1-7] several new high-temperature superconductors have been synthesized in the Tl-Ca-Ba-Cu-O system, including $Tl_2Ca_2Ba_2Cu_3O_{10\pm x}$, which displays the highest superconducting transition temperature yet found, $T_c=125$ K.[3] In this article we present data on the structures and superconducting properties of six compounds of the form $Tl_mCa_{n-1}Ba_2Cu_nO_{2(n+1)+m}$, where $m=1$ or 2 and $n=1$, 2, or 3. The structures consist of copper perovskitelike blocks containing 1, 2, or 3 CuO_2 planes separated by one or two Tl-O layers. These compounds thus form a model family of structures in which both the size and separation of the copper blocks can be independently varied. We present data that establish that the superconducting transition temperature increases with the number of CuO_2 planes in the perovskitelike block for both the Tl-O monolayer and bilayer compounds. For each pair of compounds ($m=1$, 2) with the same number of CuO_2 planes (same n), the transition temperature is 15–20 K lower in the material with single Tl-O layers. Variations in the transition temperatures in the double and triple CuO_2 layer compounds are observed to correlate with increased densities of intergrowths of related structures.

The samples were prepared by thoroughly mixing suitable amounts of Tl_2O_3, CaO, BaO_2, and CuO, and forming a pellet of this mixture under pressure. The pellet was then wrapped in gold foil, sealed in a quartz tube containing slightly less than 1 atm of oxygen, and baked for approximately 3 h at $\simeq 880\,^\circ$C. A wide range of starting compositions was studied. In most cases the resulting pellet was comprised of several phases. However, for certain ranges of starting compositions, the pellets contained only one superconducting phase of the form $Tl_mCa_{n-1}Ba_2Cu_nO_{2(n+1)+m}$ together with minor amounts ($< \simeq 20\%$) of insulating oxides such as those of Cu, Ca-Cu, Ba-Cu, and Tl-Ba. The relative amounts of each phase depended on the annealing time and temperature and the rate of cooling from this temperature. In particular, for slow cooling rates ($\simeq 100\,^\circ$C/h) the composition of the major $Tl_mCa_{n-1}Ba_2Cu_nO_{2(n+1)+m}$ phase more closely matched that of the starting composition. The composition and microstructure of the pellets were determined from complementary powder x-ray diffraction, electron microprobe, electron diffraction, and high-resolution transmission electron microscopy (TEM) studies. The superconducting properties of each pellet were examined by resistivity and dc Meissner susceptibility studies. The latter was measured with a SHE SQUID magnetometer. Cooling in a field of 100 Oe, the magnitude of the Meissner susceptibility at 5.5 K ranged from 10% to 35% of the susceptibility of a perfect diamagnet of the same volume, neglecting small demagnetizing corrections. The magnitude of the diamagnetic shielding signal is very dependent on the distribution of the normal and superconducting phases within the multiphase pellets and in most cases did not give useful information. The susceptibility data revealed that for some pellets the presence of a minority superconducting phase resulted in the resistance of the pellet dropping to zero at substantially higher temperatures than the T_c of the majority superconducting phase. This type of behavior emphasizes the importance of determining the transition temperature from a flux exclusion measurement in this complex quinary system. These results are summarized in Table I.

We have previously described the preparation and properties of the three members of the $Tl_mCa_{n-1}Ba_2Cu_nO_{2(n+1)+m}$ family, namely $Tl_2Ca_2Ba_2Cu_3O_{10}$ (2:2:2:3),[3] $Tl_2Ca_1Ba_2Cu_2O_8$ (2:1:2:2),[3] and $Tl_1Ca_2Ba_2Cu_3O_9$ (1:2:2:3),[4] which display superconducting transition temperatures of 125, 108, and 110 K, respectively. By systematically varying the starting composition of the pellets, the related compounds, $Tl_2Ca_0Ba_2Cu_1O_x$ (2:0:2:1), $Tl_1Ca_0Ba_2Cu_1O_x$ (1:0:2:1), and $Tl_1Ca_1Ba_2Cu_2O_x$ (1:1:2:2) were synthesized. The unit cells for each phase

TABLE I. Summary of properties of $Tl_mCa_{n-1}Ba_2Cu_nO_x$

Conc. ratio	Relative composition Tl	Ca	Ba	Cu	O	Symmetry	Lattice parameters a (Å)	c (Å)	Superlattice wave vector (**k**)	T_c (K)
						$Tl_1Ca_{n-1}Ba_2Cu_nO_x$				
1:0:2:1	1.2	0.0	2	0.7	4.8	*P4/mmm*	3.869(2)	9.694(9)	a	b
1:1:2:2	1.1	0.9	2	2.1	7.1	*P4/mmm*	3.8505(7)	12.728(2)	⟨0.29,0,0.5⟩	65–85
1:2:2:3	1.1	0.8	2	3.0	9.7	*P4/mmm*	3.8429(6)	15.871(3)	⟨0.29,0,0.5⟩	100–110
						$Tl_2Ca_{n-1}Ba_2Cu_nO_x$				
2:0:2:1	1.9	0.0	2	1.1	6.4	*F/mmm*[c]	$a=5.445(2)$ $b=5.492(1)$	23.172(6)	$\langle\overline{0.08},0.24,1\rangle$[c]	b
2:0:2:1[d]	1.8	0	2	1.1	6.4	*F/mmm*[c]	$a=5.4634(3)$ $b\sim a$	23.161(1)	$\langle\overline{0.08},0.24,1\rangle$[c]	20
2:0:2:1	1.8	0.02	2	1.1	6.3	*I4/mmm*	3.8587(4)	23.152(2)	$\langle\overline{0.16},0.08,1\rangle$[e]	15–20
2:1:2:2	1.7	0.9	2	2.3	8.1	*I4/mmm*	3.857(1)	29.39(1)	⟨0.17,0,1⟩	95–108
2:2:2:3	1.6	1.8	2	3.1	10.1	*I4/mmm*	3.822(4)	36.26(3)	⟨0.17,0,1⟩	118–125

[a]No superlattice spots observed.
[b]Nonmetallic or weakly metallic samples with no superconducting transition observed in resistivity and magnetic susceptibility studies for temperatures down to 4.2 K.
[c]The symmetry of the structure is *orthorhombic* if the observed superlattice is ignored. Taking the superlattice into account lowers the symmetry to *monoclinic*.
[d]Sample prepared from a Cu-rich starting composition, $Tl_2Ba_2Cu_2$.
[e]The superstructure is identical to that for the orthorhombic 2:0:2:1 polymorph.

were determined from powder x-ray diffraction patterns extending from $2\theta=3°$ to 70° and verified by electron diffraction studies. These studies showed that all of the $Tl_mCa_{n-1}Ba_2Cu_nO_{2(n+1)+m}$ compounds have tetragonal cells at room temperature. The $Tl_1Ca_{n-1}Ba_2Cu_nO_{2n+3}$ compounds contain Tl-O monolayers, resulting in primative tetragonal cells, whereas the $Tl_2Ca_{n-1}Ba_2Cu_nO_{2n+4}$ compounds contain Tl-O bilayers, resulting in body-centered tetragonal cells. The lattice parameters and symmetries of the various structures are included in Table I. As discussed later, the 2:0:2:1 compound also has an orthorhombic polymorph. As shown in Fig. 1, each oxide has a single peak in the low-angle portion ($3° \leq 2\theta \leq 10°$) of its x-ray diffraction pattern which results from the large c/a ratio in each structure. These peaks, (001) for $m=1$ and (002) for $m=2$, serve as fingerprints with which each of the compounds within the

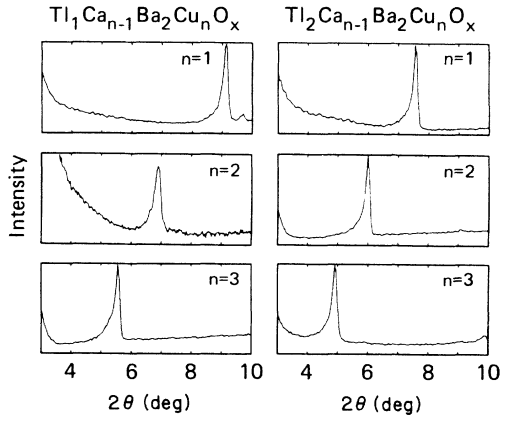

FIG. 1. Low-angle section of the powder x-ray diffraction patterns for the six phases $Tl_mCa_{n-1}Ba_2Cu_nO_{2(n+1)+m}$ ($m=1$, 2; $n=1$, 2, 3).

$Tl_mCa_{n-1}Ba_2Cu_nO_{2(n+1)+m}$ family can be uniquely identified. The peak systematically shifts to lower angles as n increases within both the $Tl_1Ca_{n-1}Ba_2Cu_nO_{2n+3}$ and $Tl_2Ca_{n-1}Ba_2Cu_nO_{2n+4}$ families, consistent with an expansion of the unit cell along the c axis by the addition of extra CuO_2 and Ca planes. The peaks are in all cases at lower angles in the $Tl_2Ca_{n-1}Ba_2Cu_nO_{2n+4}$ compounds compared to the corresponding $Tl_1Ca_{n-1}Ba_2Cu_nO_{2n+3}$ compound, consistent with the increased number of Tl-O layers in the $Tl_2Ca_{n-1}Ba_2Cu_nO_{2n+4}$ compounds. The peaks are asymmetrically broadened to low angles because of geometrical aberrations in the focusing condition resulting from the flat specimens used.[8] The arrangement of the cations in the various compounds is shown in Fig. 2. The positions of the oxygen atoms are inferred by comparison with related structures in the $La_{2-x}Sr_xCuO_4$, $YBa_2Cu_3O_x$, and $Bi_2Sr_2Ca_1Cu_2O_x$ families.[9–11] The six structures are comprised of Cu perovskitelike blocks containing one, two, or three CuO_2 planes sandwiched between Tl-O monolayers (1:0:2:1, 1:1:2:2, and 1:2:2:3 compounds) or bilayers (2:0:2:1, 2:1:2:2, 2:2:2:3 compounds). The Ba cations are located in planes adjacent to the Tl-O unit and the Ca cations form planes within the interior of the Cu perovskitelike unit.

Since the preparation, structure, and properties of the double and triple CuO_2 layer oxides appear to be much less complex than those of the single CuO_2 layer oxides for both the monolayer and bilayer Tl-O compounds, we will discuss these groups of compounds separately. As described earlier, for each of the $n=2$ and $n=3$ compounds a single tetragonal structure was found. An important structural feature of these compounds observed by TEM, scanning electron microscopy (SEM), and electron microprobe studies are intergrowths of structures related to the primary phase by the addition or removal of CuO_2 or Tl-O layers. For some samples SEM images showed contrast striations $\simeq$5–10 μm in width within individual

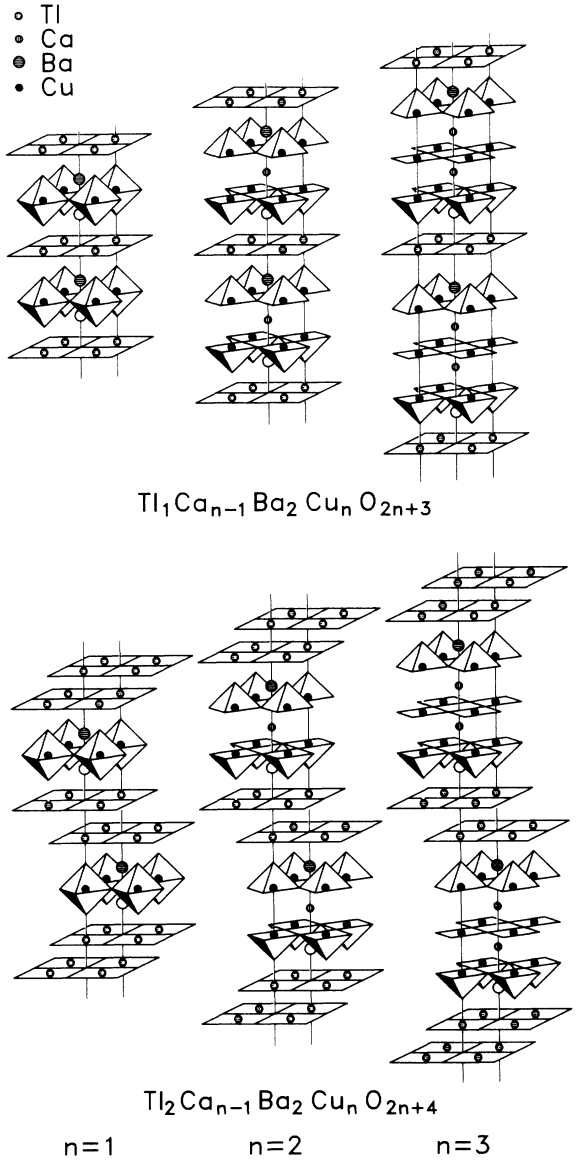

FIG. 2. Nominal structures of the six $Tl_mCa_{n-1}Ba_2Cu_nO_{2(n+1)+m}$ phases for $n=1$, 2 and $m=1$, 2, 3.

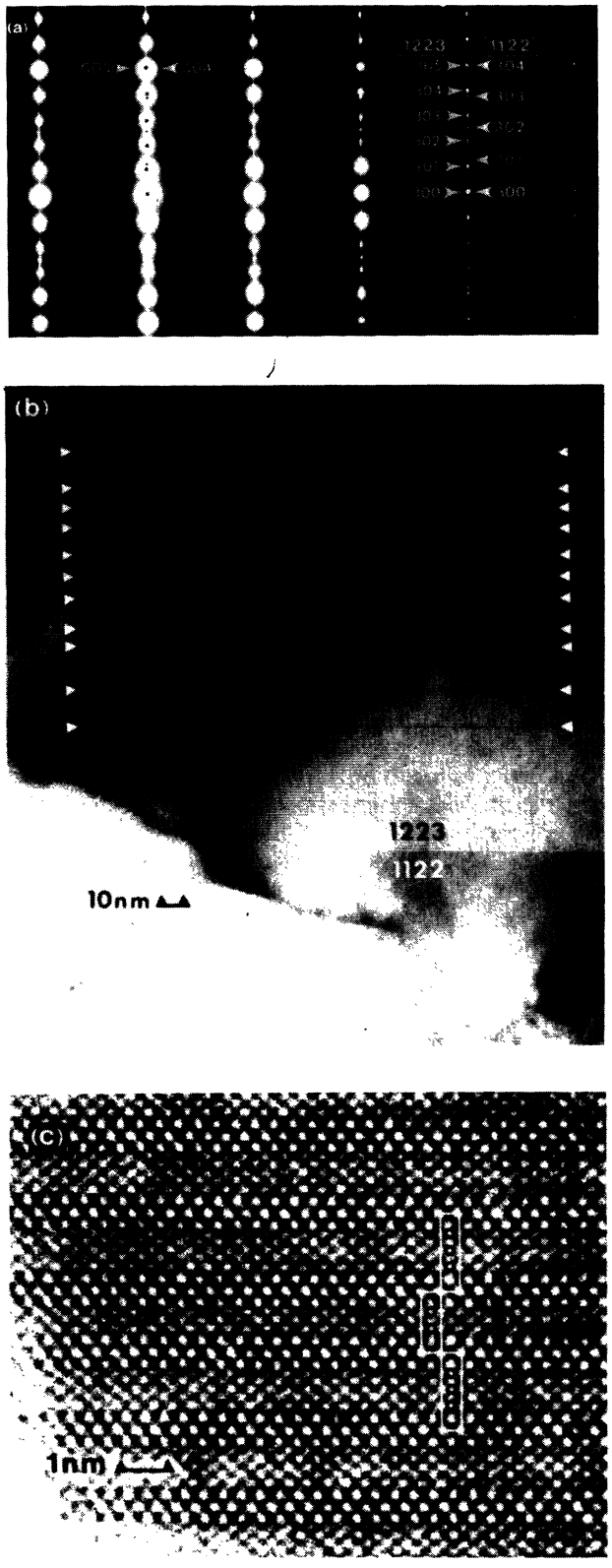

FIG. 3. (a) [010] selected area diffraction (SAD) pattern and (b) corresponding image of crystallites containing regions of 1:2:2:3 and 1:1:2:2. The arrows in (b) denote unit-cell thick intergrowths of 1:1:2:2 in 1:2:2:3. (c) High-resolution transmission electron micrograph of one unit-cell thick 1:1:2:2 intergrowth in 1:2:2:3.

grains which result from intergrowths of regions with different proportions of heavy atoms. TEM studies revealed the existence of intergrowths on much finer length scales, as demonstrated in Fig. 3 for a sample prepared from a starting composition of $Tl_{0.85}Ca_1Ba_2Cu_2$. Figure 3(a) shows a selected area diffraction pattern along b^* which indicates that this grain contains both 1:1:2:2 and 1:2:2:3 phases. Indeed Meissner data on this sample [included in Fig 4(d)] indicate two superconducting transitions with $T_c \simeq 65$ and $\simeq 105$ K, consistent with the presence of extended regions of two distinct phases. Coincidently, the c lattice parameters of the 1:1:2:2 and 1:2:2:3 phases are almost exactly in the ration of 4/5 so that every fifth 1:2:2:3 $h0l$ spot coincides with every fourth 1:1:2:2 $h0l$ spot in Figure 3(a). High-resolution TEM micrographs in Figs. 3(b) and 3(c) show intergrowths of the

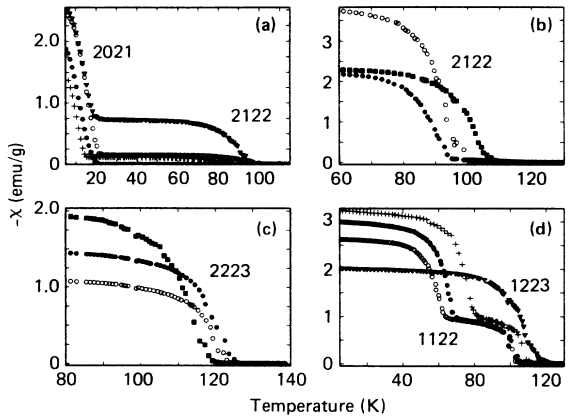

FIG. 4. Meissner susceptibility vs temperature for an applied field of 100 Oe for materials with starting cation composition, (a) $Tl_2Ba_2Cu_2$ (●), $Tl_2Ca_{0.05}Ba_2Cu_{1.05}$ (○,+), and $Tl_2Ca_{0.15}Ba_2Cu_{2.15}$ (▼); (b) $Tl_1Ca_2Ba_2Cu_3$ (●), $Tl_2Ca_1Ba_2Cu_2$ (○), and $Tl_{2.25}Ca_1Ba_2Cu_2$ (■); (c) $Tl_1Ca_2Ba_2Cu_3$ (■), $Tl_1Ca_{2.5}Ba_1Cu_3$ (○), and $Tl_1Ca_3Ba_1Cu_3$ (●); (d) $Tl_{0.85}Ca_1Ba_2Cu_2$ (○), $Tl_1Ca_1Ba_2Cu_2$ (●,+), and $Tl_{0.85}Ca_2Ba_2Cu_3$ (▼). The phases present in the pellet giving rise to the diamagnetic susceptibility are (a) 2:0:2:1 and 2:1:2:2, (b) 2:1:2:2, (c) 2:2:2:3, and (d) 1:1:2:2 and 1:2:2:3.

1:1:2:2 and 1:2:2:3 phases on length scales extending from $\simeq 1\mu$m down to one unit cell. The intergrowths are randomly distributed along the stacking axis. Isolated intergrowths comprising four CuO_2 planes were found in some samples (see Fig. 5) but no evidence was found for extended intergrowths comprising greater than three CuO_2 layers in these or other samples especially prepared from Cu- and Ca-rich starting compositions. A second type of intergrowth was observed in samples of the 1:2:2:3 phase in which an extra Tl-O plane was occasionally inserted between the Cu perovskitelike units, creating local regions of the 2:2:2:3 phase. Microprobe data show that the Tl content is systematically high in the compounds containing single Tl-O layers and systematically low in those compounds with Tl-O bilayers (see Table I) thus suggesting that intergrowths of Tl-O monolayers in the Tl-O bilayers materials and Tl-O bilayers in the Tl-O monolayer compounds are a general feature of these materials.

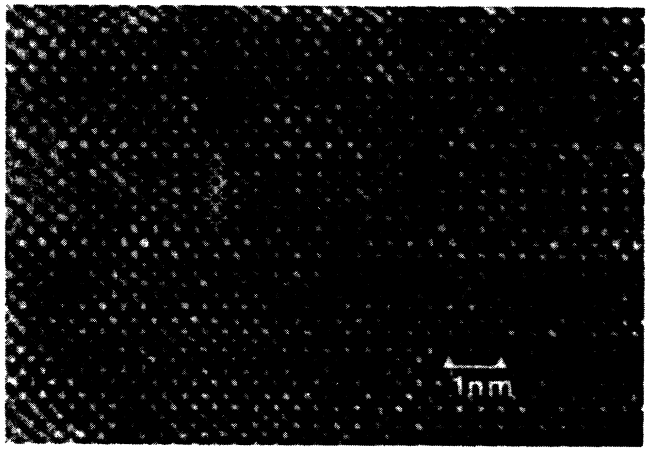

FIG. 5. High-resolution TEM image of an isolated four-CuO_2-layer intergrowth. The markers denote the positions of the Cu columns.

Meissner data (see Fig. 4) established that T_c can take a range of values for all of the double and triple CuO_2 layer compounds— $T_c \simeq 95$–108 K for 2:1:2:2, $T_c \simeq 118$–125 K for 2:2:2:3, $T_c \simeq 65$–85 K for 1:1:2:2, and $T_c \simeq 100$–110 K for 1:2:2:3. For a given compound, x-ray diffraction and microprobe studies did not detect any obvious difference between the samples with different transition temperatures. TEM studies, however, showed a clear correlation between the density of intergrowths and T_c. For the 2:1:2:2, 2:2:2:3, and 1:2:2:3 phases the material with no intergrowths displayed the highest transition temperature, whereas for the 1:1:2:2 compound the sample with the lowest density of intergrowths had the lowest T_c. As the density of intergrowths increased we observed that T_c systematically decreases or increases, respectively. It is possible that the structural or electronic modifications caused by the intergrowths are directly responsible for the decreased transition temperatures. Alternatively the presence of the intergrowths may simply reflect a means whereby the system accommodates, to some extent, off-stoichiometry in the cation sites which in turn may influence T_c. It is difficult to determine whether it is the local change in structure or composition which is responsible for the decrease in T_c since these are concurrent changes.

A second important structural feature found in all of the double and triple CuO_2 layer compounds is the presence of weak superlattice reflections in the selected area electron diffraction patterns. These reflections are considerably weaker than those previously found in the $Bi_2Sr_2Ca_1Cu_2O_x$ compound[12–16] and indicate different structural modulations than those in the $Bi_2Sr_2Ca_1Cu_2O_x$ compound. The patterns can be described by a set of symmetry-related wave vectors, **k**. Each wave vector describes a pair of reflections symmetrically disposed a reciprocal distance $|\mathbf{k}|$ along **k** on either side of each Bragg peak, which would be consistent with a sinusoidal modulation of the charge density along this direction.[17] The possibility that each **k** corresponds to a different crystal variant with lowered symmetry is unresolved. The Tl-O monolayer and bilayer families each display a distinctive pattern of superlattice reflections, shown schematically in Figs. 6(a) and 6(b). One example of electron diffraction patterns showing the superlattice reflections is given in Fig. 7 for the 1:1:2:2 phase.

The structure and properties of the single CuO_2 layer compounds are more sensitive to the preparation conditions than those of the double and triple CuO_2 layer compounds. When prepared from a $Tl_2Ba_2Cu_1$ starting composition, the 2:0:2:1 compound has a face-centered orthorhombic cell and is not superconducting. The material is heavily twinned with twin planes of {110} type in the orthorhombic cell. This cell is related to the tetragonal cell by a rotation of $\simeq 45°$ about the c axis with a and b increased in size by a factor of $\simeq\sqrt{2}$. However when the 2:0:2:1 compound is prepared from a Cu-rich starting composition, $Tl_2Ba_2Cu_2$, the compound is superconduct-

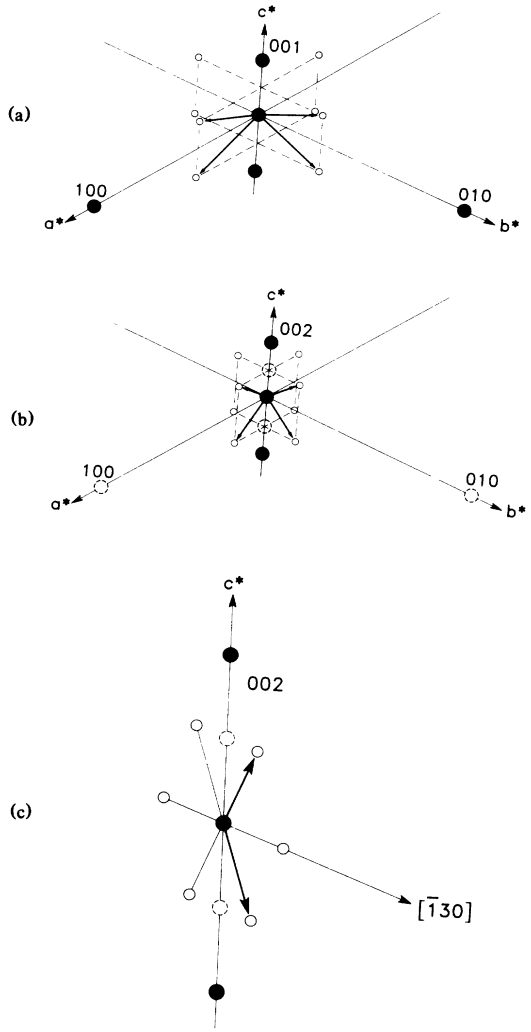

FIG. 6. Schematic diagram of the arrangement of superlattice reflections about the fundamental reflections for (a) the 1:1:2:2 and 1:2:2:3 phases, (b) the 2:1:2:2 and 2:2:2:3 phases, (c) the 2:0:2:1 phase. The fundamental reflections are shown as solid circles, and those which are systematically absent are shown as dashed circles. The superstructure is shown by open circles and the corresponding wave vectors by bold arrows.

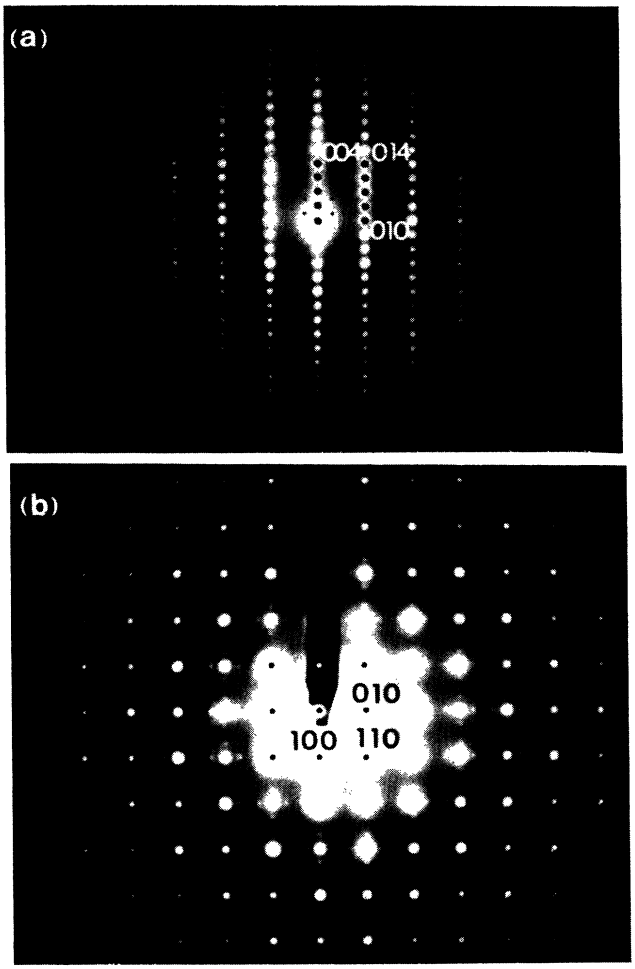

FIG. 7. (a) [100] and (b) [001] selected area diffraction patterns from crystallites of 1:1:2:2 showing superlattice reflections.

ing at $\simeq$20 K. While x-ray data indicate the structure is pseudotetragonal, transmission electron micrographs reveal a tweed pattern which is consistent with local orthorhombic distortion. A tetragonal polymorph with no evidence from TEM studies of either an average or local orthorhombic distortion can be formed by preparing the compound from a pellet containing a small amount of Ca (Tl:Ca:Ba:Cu $=2:y:2:1+y$, with $y\simeq 0.05$–0.15). This polymorph is also superconducting with a T_c which is independent of the amount of Ca in the starting composition but weakly dependent on the annealing time—T_c $\simeq$15 and 20 K for anneal times at 880 °C of 3 and 9 h, respectively. As suggested by the Meissner data in Fig. 4(a) these pellets contain, in addition to the tetragonal 2:0:2:1 phase, a substantial amount of the 2:1:2:2 phase which increases as the proportion of Ca in the starting composition is increased. There is a sufficient amount of this phase that the resistance of these pellets actually drops to zero at $T_c\simeq 100$ K. The Meissner data in Fig. 4(a) show that for $y\simeq 0.05$ the ratio of 2:1:2:2 to 2:0:2:1 is about 8% and for $y\simeq 0.15$ the ratio is increased to $\simeq$30%. Electron microprobe analysis shows that only a small amount of Ca ($\simeq$0.2 at.%) is incorporated into the 2:0:2:1 grains and consequently the role of the Ca doping in changing the structure and properties of the 2:0:2:1 material is unclear. Moreover there are reports that the 2:0:2:1 phase can be prepared without Ca with a transition temperature as high as $\simeq$85 K.[5] Both polymorphs of the 2:0:2:1 structures display a similar superlattice with an approximate wave vector, $\mathbf{k}=[\overline{0.08},0.24,1]$ in the orthorhombic setting. Taking the superlattice into account lowers the symmetry of both the orthorhombic and tetragonal structures to monoclinic with the c axis being unique. As shown in Fig. 8 this superstructure is different from those found in the double and triple CuO_2 layer compounds.

The other member of the $Tl_mCa_{n-1}Ba_2Cu_nO_{2(n+1)+m}$ family which contains single CuO_2 layers, the 1:0:2:1 phase, has a primitive tetragonal cell and is not superconducting for the wide range of preparative conditions considered in this study, including growth from Cu-rich or Ca-doped starting compositions. No superstructures have been observed in these crystals so far.

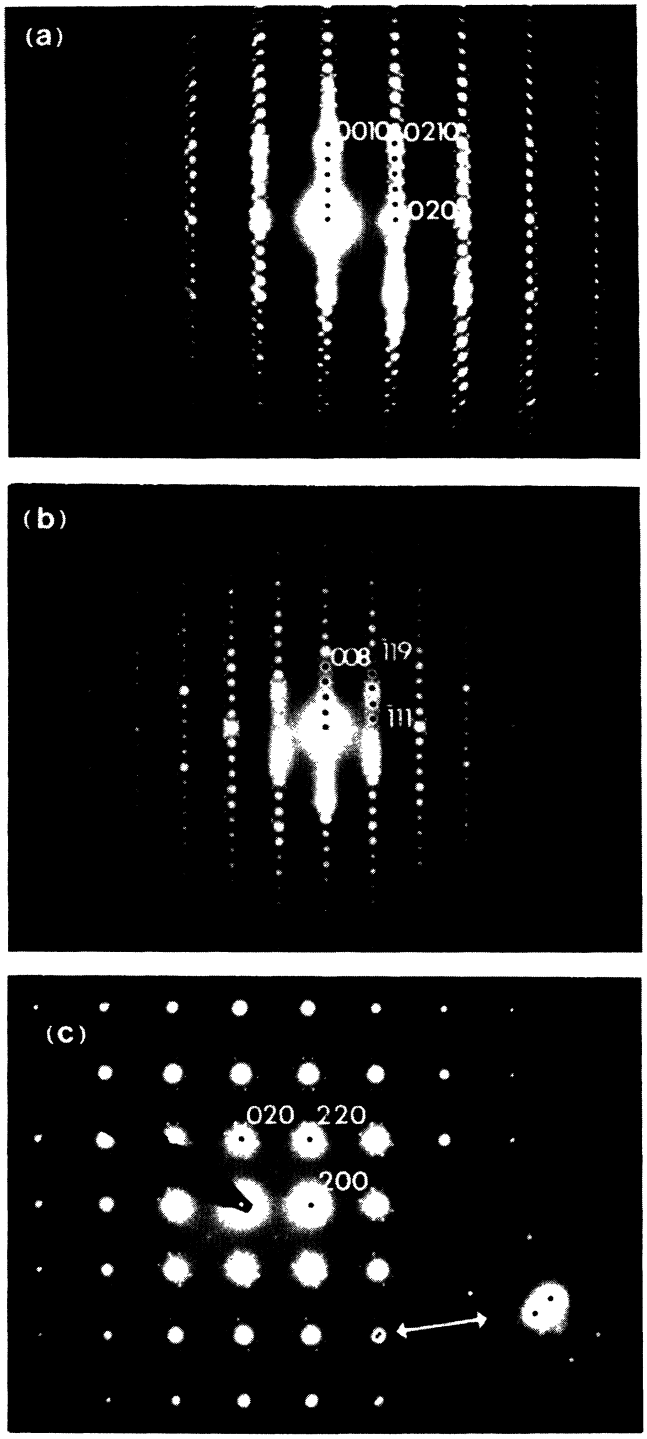

FIG. 8. (a) [100], (b) [110], and (c) [001] selected area diffraction patterns from a crystallite of 2:0:2:1.

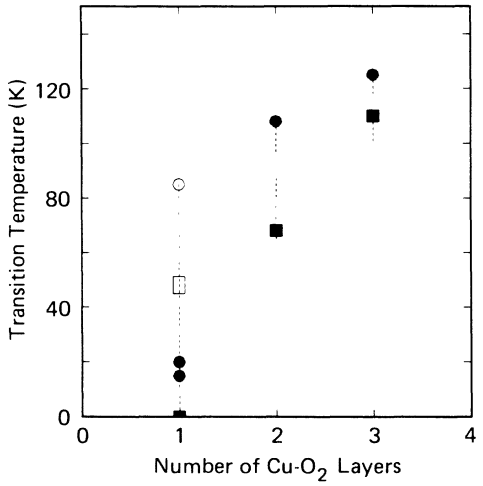

FIG. 9. Dependence of T_c on the number of CuO_2 planes within the Cu perovskitelike unit for the $Tl_1Ca_{n-1}Ba_2Cu_nO_{2n+3}$ (■) and $Tl_2Ca_{n-1}Ba_2Cu_nO_{2n+4}$ (●, this work; ○, Ref. 5) series of compounds. The dashed vertical lines correspond to the variations in T_c found for each phase. □ corresponds to data for (Tl, Bi)$_1$(Ca,Sr)$_2$Cu$_1$O$_x$ (Ref. 21).

As shown in Table I there is no obvious correlation of superlattice structure with the superconducting properties of the $Tl_mCa_{n-1}Ba_2Cu_nO_{2(n+1)+m}$ compounds. Note that in the closely related compound, $Bi_2Sr_1Ca_2Cu_2O_x$, it has recently been proposed that the observed incommensurate superlattice corresponds to a distortion of both the Bi-O and CuO_2 planes resulting from ordered vacancies on the Sr sites.[16] The vacancies are postulated to determine the carrier density on the CuO_2 planes and so influence the T_c in a manner similar to that first noted by Schafer, Penney, and Olsen for the $La_{2-x}Sr_xCuO_{4-y}$ compounds.[18] The number of different superlattice structures found in the Tl-Ca-Ba-Cu-O system provides a more extensive basis with which to test such hypotheses. Indeed it may be significant that, as shown in Table I, there are important variations in stoichiometry away from the ideal stoichiometries expected for the various $Tl_mCa_{n-1}Ba_2Cu_nO_{2(n+1)+m}$ phases. In particular, the [Tl]/[Ba] ratio is higher for the $n=1$ compounds compared to those for $n=2$ and $n=3$. Band-structure calculations of both the $Tl_mCa_{n-1}Ba_2Cu_nO_{2(n+1)+m}$ compounds and $Bi_2Sr_1Ca_2Cu_2O_x$ indicate that the stoichiometry of the Tl-O and Bi-O layers would have a profound impact on the carrier density in these materials.[19,20] The extent of off-stoichiometry on the cation or the oxygen sites in the Tl-Ca-Ba-Cu-O phases requires further study. Note also that one group has recently prepared a complex material of the form (Tl,Bi)$_1$(Ca,Sr)$_2$Cu$_1$O$_x$ with the 1:0:2:1 structure which appears to superconduct at temperatures of up to 50 K (Ref. 21). The variation of properties of the single CuO_2 layers compounds provides a fertile area for further study and highlights the difficulties in preparing these multicomponent oxides in a controlled manner.

In conclusion, these studies have shown that the superconducting transition temperature increases with the number of CuO_2 planes in the perovskitelike unit for both the $Tl_1Ca_{n-1}Ba_2Cu_nO_{2n+3}$ and $Tl_2Ca_{n-1}Ba_2Cu_nO_{2n+4}$ structures (Fig. 9). A similar dependency is found in both series of compounds with an increased spread of T_c as the number of CuO_2 planes is reduced. The range of T_c in the double and triple CuO_2 layer compounds correlates with the density of intergrowth defects. No such defects have ben observed so far in the single CuO_2 layer compounds,

even when doped with Ca. One might speculate that in this case the variation in transition temperature may result from variations in cation or oxygen site occupancy. The increase in T_c as n increases may be accounted for by various theories, including several based on the BCS theory[19] and others invoking more exotic mechanisms such as the resonating-valence-bond model.[22] The variety of structures and properties in the Tl-Ca-Ba-Cu-O system provides a model family of compounds with which various theories of high-temperature superconductivity can be evaluated.

We are indebted to S. J. La Placa, F. Herman, and J. B. Torrance for many useful discussions. We thank C. C. Torardi, R. B. Flippen, and R. M. Hazen for discussions regarding the 2:0:2:1 compound. We are grateful to Professor Sinclair at Stanford for the use of his electron microscope.

[1]Z. Z. Sheng and A. M. Hermann, Nature (London) **332**, 138 (1988); **332**, 55 (1988).

[2]R. M. Hazen, L. W. Finger, R. J. Angel, C. T. Prewitt, N. L. Ross, C. G. Hadidiacos, P. J. Heaney, D. R. Veblen, Z. Z. Sheng, A. El Ali, and A. M. Hermann, Phys. Rev. Lett. **60**, 1657 (1988).

[3]S. S. P. Parkin, V. Y. Lee, E. M. Engler, A. I. Nazzal, T. C. Huang, G. Gorman, R. Savoy, and R. Beyers, Phys. Rev. Lett. **60**, 2539 (1988).

[4]S. S. P. Parkin, V. Y. Lee, A. I. Nazzal, R. Savoy, R. Beyers, and S. J. La Placa, Phys. Rev. Lett. **61**, 750 (1988).

[5]C. C. Torardi, M. A. Subramanian, J. C. Calabrese, J. Gopalakrishnan, K. J. Morrissey, T. R. Askew, R. B. Flippen, U. Chowdry, and A. W. Sleight, Science **240**, 631 (1988).

[6]M. A. Subramanian, J. C. Calabrese, C. C. Torardi, J. Gopalakrishnan, T. R. Askew, R. B. Flippen, K. J. Morrissey, U. Chowdry, and A. W. Sleight, Nature (London) **332**, 420 (1988).

[7]S. Kondoh, Y. Ando, M. Onoda, and M. Sato, Solid State Commun. **65**, 1329 (1988).

[8]W. Parrish, *X-ray and Electron Methods of Analysis* (Plenum, New York, 1968).

[9]J. M. Tarascon, Y. Le Page, P. Barboux, B. G. Bagley, L. H. Greene, W. R. McKinnon, G. W. Hull, M. Giroud, and D. M. Hwang, Phys. Rev. B **37**, 9382 (1988).

[10]S. A. Sunshine, T. Siegrist, L. F. Schneemeyer, D. W. Murphy, R. J. Cava, B. Batlogg, R. B. van Dover, R. M. Fleming, S. H. Glarum, S. Nakahara, R. Farrow, J. J. Krajewski, S. M. Zahurak, J. V. Waszczak, J. H. Marshall, P. Marsh, L. W. Rupp, and W. F. Peck, Phys. Rev. B **38**, 893 (1988).

[11]J. B. Torrance, Y. Tokura, S. J. LaPlaca, T. C. Huang, R. J. Savoy, and A. I. Nazzal, Solid State Commun. **66**, 703 (1988).

[12]T. M. Shaw, S. A. Shivanshankar, S. J. LaPlaca, J. J. Cuomo, T. R. McGuire, R. A. Roy, K. H. Kelleher, and D. S. Yee, Phys. Rev. B **37**, 9856 (1988).

[13]D. R. Veblen, P. J. Heaney, R. J. Angel, L. W. Finger, R. M. Hazen, C. T. Prewitt, N. L. Ross, C. W. Chu, P. H. Hor, and R. L. Meng, Nature (London) **332**, 334 (1988).

[14]E. A. Hewat, M. Dupuy, P. Bordet, J. J. Capponi, C. Chaillout, J. L. Hodeau, and M. Marezio, Nature (London) **333**, 53 (1988).

[15]H. W. Zandbergen, Y. K. Huang, M. J. V. Menken, J. N. Li, K. Kadowaki, A. A. Menovsky, G. van Tendeloo, and S. Amelinckx, Nature (London) **332**, 620 (1988).

[16]P. L. Gai and P. Day (unpublished).

[17]P. M. De Wolff, Acta Crystallogr. Sec. A **30**, 777 (1974).

[18]M. W. Shafer, T. Penney, and B. L. Olsen, Phys. Rev. B **36**, 4047 (1987).

[19]M. S. Hybertson and L. F. Mattheiss, Phys. Rev. Lett. **60**, 1661 (1988).

[20]F. Herman, R. V. Kasowski, and W. Y. Hsu, Phys. Rev. B **38**, 204 (1988); F. Herman, R. V. Kasowski, S. J. La Placa, and S. S. P. Parkin (unpublished).

[21]P. Haldar, A. Roig-Janicki, S. Sridhar, and B. C. Giessen (unpublished).

[22]J. M. Wheatley, T. C. Hsu, and P. W. Anderson, Nature (London) **333**, 121 (1988).

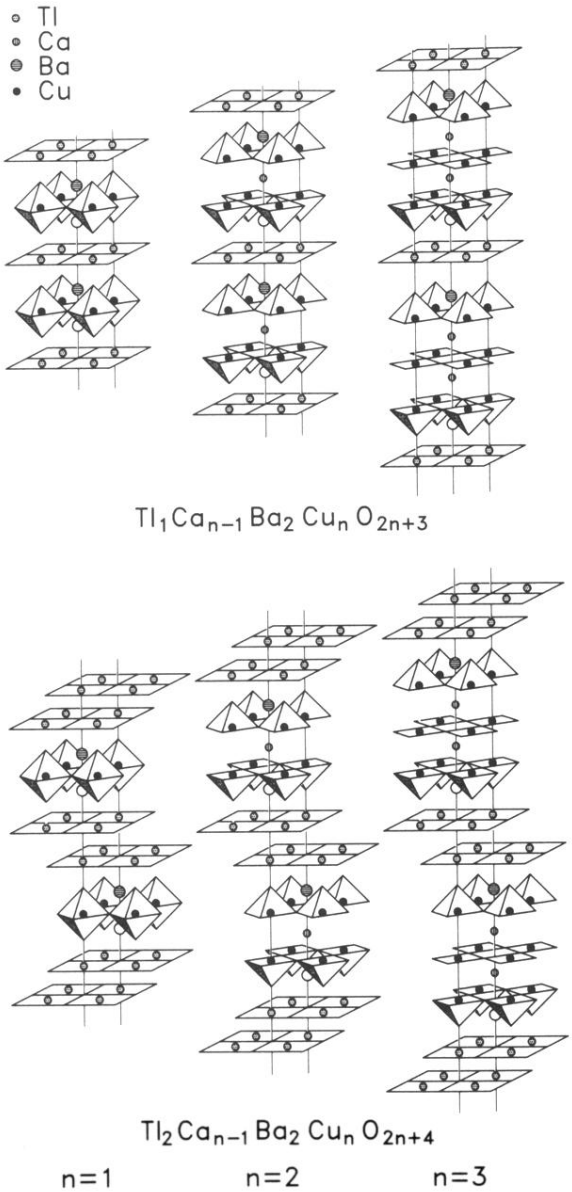

FIG. 2. Nominal structures of the six $Tl_mCa_{n-1}Ba_2Cu_nO_{2(n+1)+m}$ phases for $n=1, 2$ and $m=1, 2, 3$.

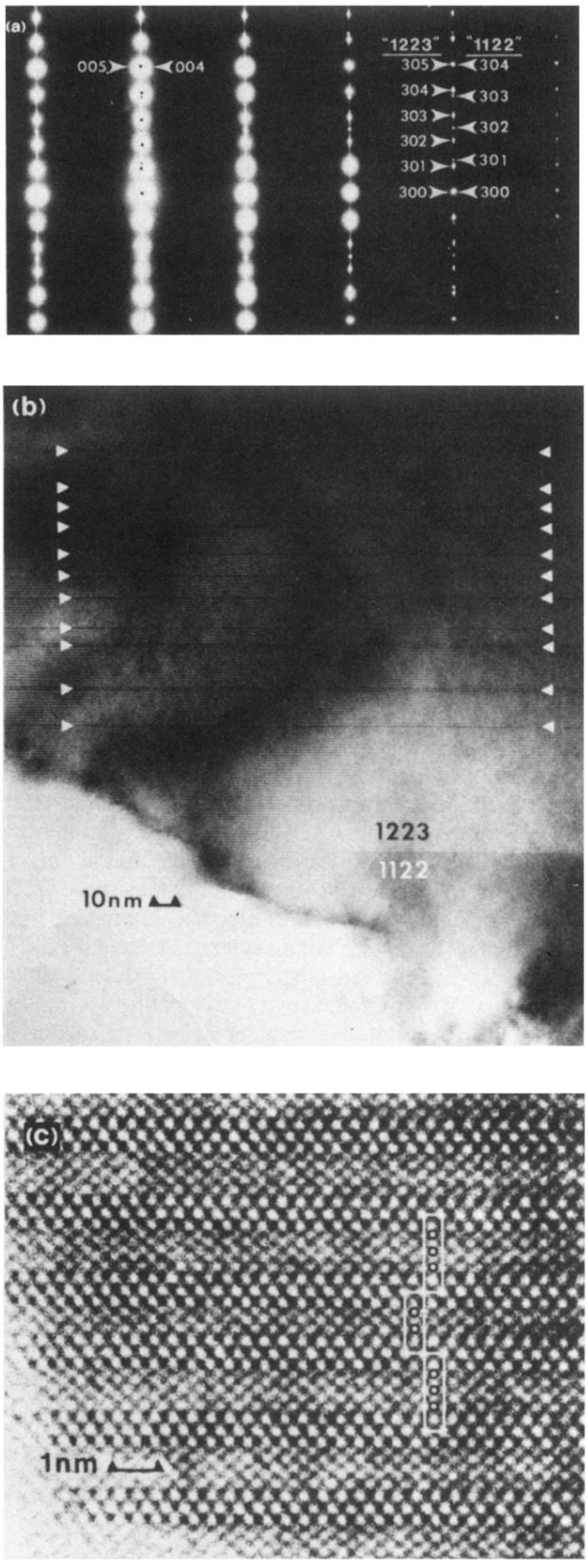

FIG. 3. (a) [010] selected area diffraction (SAD) pattern and (b) corresponding image of crystallites containing regions of 1:2:2:3 and 1:1:2:2. The arrows in (b) denote unit-cell thick intergrowths of 1:1:2:2 in 1:2:2:3. (c) High-resolution transmission electron micrograph of one unit-cell thick 1:1:2:2 intergrowth in 1:2:2:3.

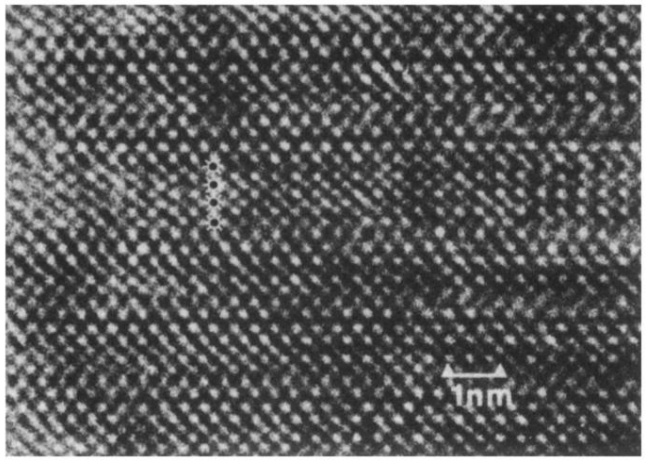

FIG. 5. High-resolution TEM image of an isolated four-CuO_2-layer intergrowth. The markers denote the positions of the Cu columns.

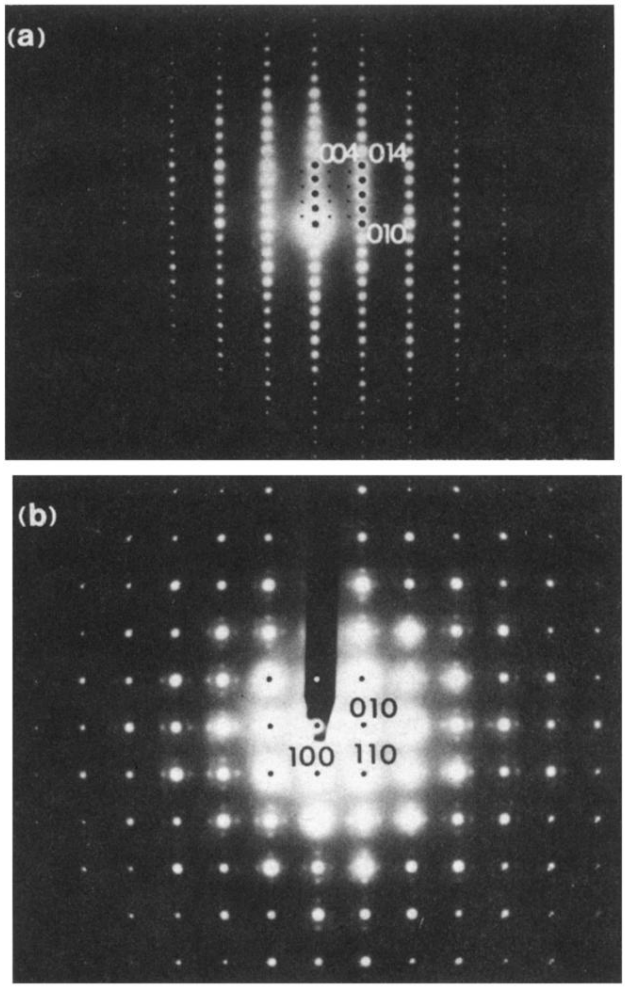

FIG. 7. (a) [100] and (b) [001] selected area diffraction patterns from crystallites of 1:1:2:2 showing superlattice reflections.

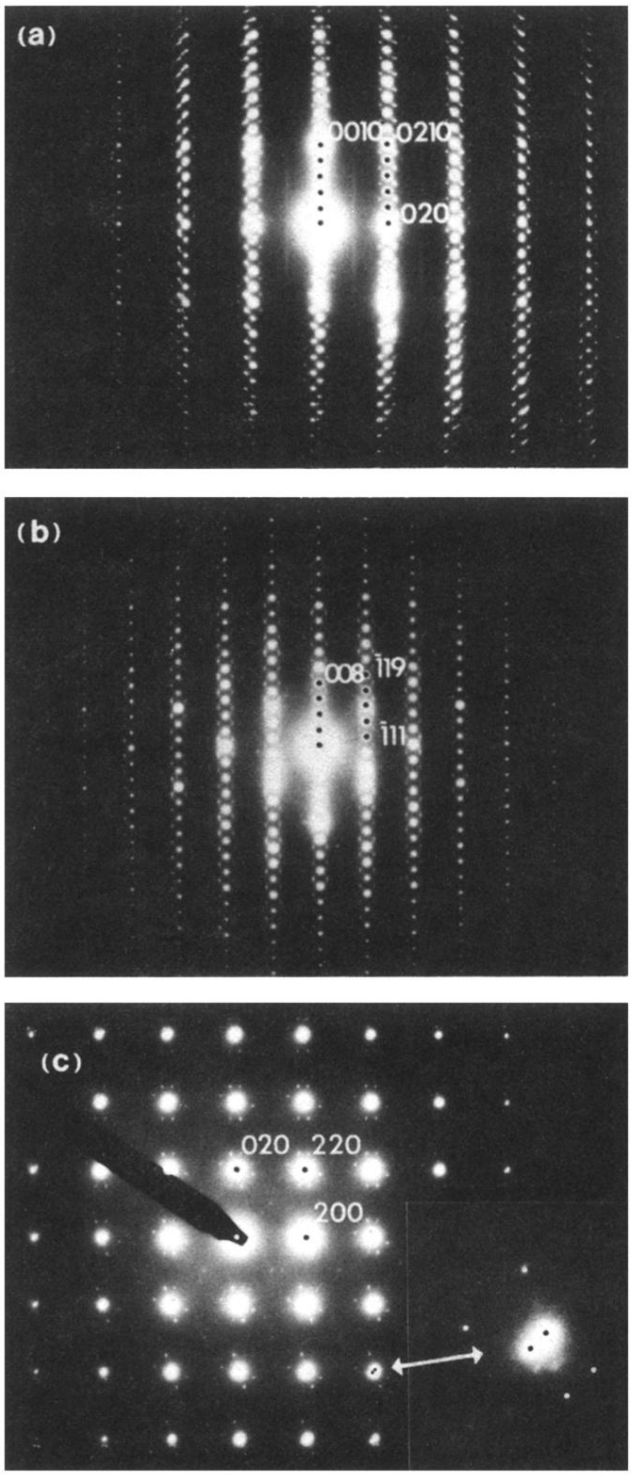

FIG. 8. (a) [100], (b) [110], and (c) [001] selected area diffraction patterns from a crystallite of 2:0:2:1.